Elucidation of the bonding in Mn(η^2-SiH) complexes by charge density analysis and T_1 NMR measurements: asymmetric oxidative addition and anomeric effects at silicon†

Wolfgang Scherer,*[a] Georg Eickerling,[a] Maxim Tafipolsky,[a] G. Sean McGrady,*[b] Peter Sirsch[b] and Nicholas P. Chatterton[c]

Received (in Berkeley, CA, USA) 12th April 2006, Accepted 17th May 2006
First published as an Advance Article on the web 7th June 2006
DOI: 10.1039/b604843a

The bonding in Mn(η^2-SiH) complexes is interpreted in terms of an asymmetric oxidative addition whose extent is controlled by the substitution pattern at the hypercoordinate silicon centre, and especially by the ligand *trans* to the η^2-coordinating SiH moiety.

Transition metal σ-bond complexes constitute a well documented class of compounds, with examples ranging from molecular dihydrogen complexes through agostic C–H systems to activated boranes.[1] They have been extensively studied by standard structural and spectroscopic techniques, as well as by quantum chemical studies, but very few experimental or theoretical approaches can provide a direct insight into the bonding in such systems. High-resolution X-ray diffraction studies combined with a topological analysis of charge densities have recently been used successfully to investigate the nature of agostic M(η^2-CH) interactions,[2] and to identify local acidic centres formed in the valence electron density of the metal as metrics for the extent of C–H activation.

Metal complexes containing (η^2-SiH) moieties act as intermediates in hydrosilation and related metal-mediated transformations. An accurate description of their bonding will assist in understanding these important processes, and will facilitate comparison of (η^2-SiH), (η^2-HH) and (η^2-CH) bonding.[1–3] The rich variety of silane ligands coordinated to the $CpMn(CO)_2$ fragment serves as a paradigm for the phenomenon. Accordingly, we have undertaken a combined experimental and theoretical charge density (CD) study of the bonding in the complexes [Cp′Mn(CO)$_2$(η^2-HSiHPh$_2$)] **1** and [Cp′Mn(CO)$_2$(η^2-HSiFPh$_2$)] **2** [Cp′ = (η^5-C$_5$H$_4$Me)], Fig. 1, whose structures have been determined accurately by neutron diffraction.[4,5]

Complexes **1** and **2** were prepared according to literature methods,[3] and crystals suitable for diffraction were obtained by repeated recrystallisation from *n*-pentane. The experimental CD for **2** was obtained by fitting a multipole model[6] to the high-resolution X-ray data,[7] compared with theoretical values from DFT calculations,[9] and analysed using Bader's 'Atoms in Molecules' (AIM) theory.[10,11]

Schubert has explored the chemical and structural features of a range of Mn(η^2-SiH) complexes, including both **1** and **2**.[3] Solution ^{1}H NMR spectra generally display a reduction in *J*(Si,H) to around one-third of that for the free silanes; proportionately greater than that observed for (η^2-HH) or (η^2-CH) bonds,[1] and implying a bonding situation intermediate between a σ-bond complex and full oxidative addition of the Si–H moiety. He(I) photoelectron spectroscopy studies provided further insight into the nature of silane coordination and led Lichtenberger and Rai-Chaudhuri to conclude that the fluoro complex **2** shows a greater charge redistribution to the Si–H σ* orbital than does the hydrido complex **1**, owing to stabilisation of the antibonding Si–H orbital by the electronegative fluorine substituent.[12] Such an effect should be reflected in the bridging Si–H bond distance. However, the neutron diffraction structures of **1** and **2** (Fig. 1) clearly reveal that the bridging Si–H bonds are identical within the range of experimental error [1.806(14) **1** *vs.* 1.802(5)[5] Å **2**]. The (η^2-Si–H) distance in each complex is significantly lengthened compared to those found in four-coordinate SiH_4 [*ca.* 1.4798(4) Å],[13a] or the hypervalent five-coordinate $[H_2SiPh_3]^-$ anion [1.593(2) and 1.602(2) Å].[13b] Furthermore, the Mn–H distance [1.575(14) Å] in **1** is also indistinguishable from that in **2** [1.569(4) Å].[5] It is remarkable that in both complexes this distance is even shorter than the typical Mn–H single bond in $HMn(CO)_5$ [1.601(16)].[14]

The long Si–H and short Mn–H distances in **1** and **2** clearly vitiate their classification as Mn(η^2-SiH) complexes at an early

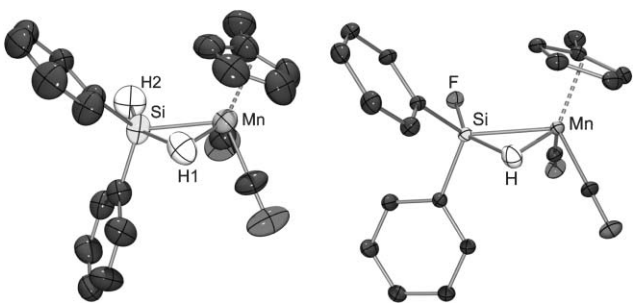

Fig. 1 Molecular structure of **1** (*left*, 295 K, neutron diffraction study) and **2** (*right*, 120 K, high-resolution X-ray study; ADP were adopted to the neutron diffraction model of ref. 5) at the 50% probability level. Only the relevant hydrogen atoms are shown.

[a]*Lehrstuhl für Chemische Physik und Materialwissenschaften, Universität Augsburg, D-86159, Augsburg, Germany. E-mail: wolfgang.scherer@physik.uni-augsburg.de; Fax: +49 0821 598 3227; Tel: +49 0821 598 3350*
[b]*Department of Chemistry, University of New Brunswick, Fredericton, N.B., Canada E3B 6E2. E-mail: smcgrady@unb.ca*
[c]*Department of Chemistry, University of Sheffield, Sheffield, UK S3 7HF*

† Electronic supplementary information (ESI) available: Geometrical and topological parameters of **2**; experimental and computational details; comparison of different multipole models; residual and deformation electron density maps. See DOI: 10.1039/b604843a

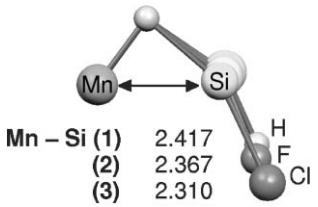

Fig. 2 Superposition of the BPW91/6-311G(d,p) optimised geometries of the Mn(η^2-SiHX) moiety in **1–3** where X = H, F, Cl, respectively; bond distances in Å.

stage of Si–H bond addition.[12a] It is therefore informative to compare the structural parameters of **1** and **2** with those of [Cp′Mn(CO)$_2$(HSiCl$_3$)][3] **3**, which has been classified on the basis of its PE spectrum as a genuine oxidative addition product[12b] with a Mn(III) centre and fully fledged Mn–Si and Mn–H bonds. However, superposition of the geometries of the optimised Mn(η^2-SiHX) moiety (X = H, F, Cl, respectively) for **1–3**, Fig. 2, clearly reveals the close structural relationship between all three complexes, with almost identical Si–H and Mn–H bond distances and H–Mn–Si angles, and does not support such classification of **3**.

According to Fig. 2, only the Mn–Si distance—the third metric characterising the [Mn–Si–H] moiety—permits discrimination between **1** and **2** and complex **3** (Mn–Si = 2.391(12) [2.417], 2.352(4)[5] [2.367] and 2.254(1)[3] [2.310] Å, respectively; theoretical values in square brackets). This implies that addition of the polar Si–H moiety to a transition metal centre might occur in an *asymmetric* manner as postulated by Schubert,[3] proceeding faster along the M–H reaction coordinate so that bond formation between the metal and the more electronegative H atom in **1–3** achieves an advanced stage while that between the metal and the more electropositive ligand Si atom lags behind. Complexes **1–3** can each then be classified as products of such asymmetric oxidative addition, but at various stages of Si–Mn bond formation.

Such a conclusion is supported by the topology of the CD, $\rho(\boldsymbol{r})$, in complexes **1–3**, through an AIM analysis. Fig. 3 shows the negative Laplacian, $L(\boldsymbol{r}) = -\nabla^2\rho(\boldsymbol{r})$, of the experimental and theoretical CD distributions for the Mn–H–Si moiety of **2**. The

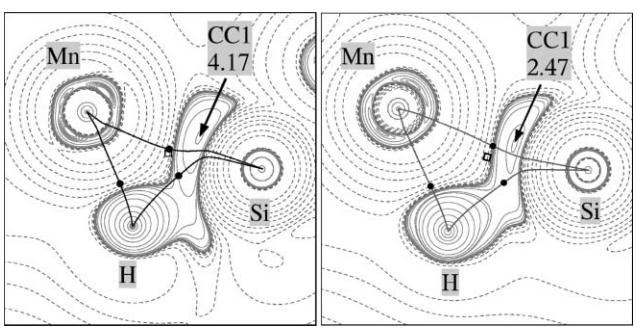

Fig. 3 $L(\boldsymbol{r})$ contour maps of the experimental (*left*) and theoretical (*right*) electron density of **2** in the Mn,H,Si plane. Contour levels are drawn at 0.001, $\pm 2.0 \times 10^n$, $\pm 4.0 \times 10^n$, $\pm 8.0 \times 10^n$ eÅ^{-5}, where n = 0, 3, ± 2, ± 1; extra levels at 11.5, 15.0, 1200 and 1500 eÅ^{-5}; positive and negative values are marked by solid and dashed lines, respectively. BCPs and RCPs are marked by closed circles and squares, respectively; the bond paths are shown by solid lines. The position and magnitude of CC1 in the valence shell of the Si atom is marked by arrows.

Table 1 Analysis of bond and ring CPs [$\rho(\boldsymbol{r}_c)$ in eÅ^{-3}, $\nabla^2\rho(\boldsymbol{r}_c)$ in eÅ^{-5} and distances in Å] in **1**, **2** and **3**

Parameter		Mn–Si	Mn–H	Si–H	Mn,Si,H RCP
r(A–B)	**1** Exp.[a]	2.391(12)	1.575(14)	1.806(14)	—
	Theory	2.417	1.565	1.804	—
	2 Exp.(N)[b]	2.352(4)	1.569(4)	1.802(5)	—
	Exp.(X)[c]	2.3509(2)	1.570[d]	1.806[d]	—
	Theory	2.367	1.566	1.817	—
	3 Theory	2.310	1.555	1.841	—
$\rho(\boldsymbol{r}_c)$	**1** Theory	—	0.76	0.52	—
	2 Exp.	0.51(3)	0.75(1)	0.53(4)	0.51(3)
	Theory	0.50	0.76	0.53	0.50
	3 Theory	0.55	0.80	0.54	0.53
$\nabla^2\rho(\boldsymbol{r}_c)$	**1** Theory	—	4.30	−1.64	—
	2 Exp.	1.37(5)	5.65(1)	−0.83(6)	1.32(5)
	Theory	0.30	4.35	−1.50	0.98
	3 Theory	0.15	3.66	−0.86	1.32

[a] Ref. 4. [b] Ref. 5. [c] This work. [d] Fixed hydrogen atom position.

Mn–Si and Si–H bond critical points (BCPs) and ring critical point (RCP) are proximal and located in a region with a rather flat electron density profile (Table 1 and Fig. 3). Since $\rho(\boldsymbol{r})$ at a BCP provides a sensitive measure of the bond strength, it appears that the Mn–Si and Si–H bonds are significantly weaker than the Mn–H bond (Table 1), in accord with the structural parameters (Fig 2). In particular, the curvature of the Si–H bond path leads the RCP and BCP almost to merge into a singularity in $\rho(\boldsymbol{r})$, a confluence characteristic of bond fission. The same is true of the Mn–Si BCP, and results in large bond ellipticities (ε). In contrast, the Mn–H bond displays a pronounced CD at the BCP and a much lower ε value; together with an almost linear bond path, this implies a stable bond (Fig. 3). Recent theoretical analyses of the CD distribution in **2**[2b] and **3**[15] predict rather similar topological features for the Mn–H–Si moiety. However, the Mn–Si BCP in **3** [$\rho(\boldsymbol{r}_c)$ = 0.55 eÅ^{-3}] appears somewhat more pronounced than that in **2** [$\rho(\boldsymbol{r}_c)$ = 0.51(3) [0.50] eÅ^{-3}; exp. [calc.]], in accord with the structural parameters reported in Fig. 2. Hence, the topology of the charge density—a direct insight into the electronic structure—also supports classification of complexes **1–3** as asymmetric oxidative addition products which differ in the extent of Mn–Si bond formation. In this respect, Bader and Matta's classification of **3** as a [Cp′Mn(CO)$_2$H]·[SiCl$_3$] adduct[15] is potentially misleading, since it rules out any *concerted* reaction mechanism leading to an oxidative addition product.

We now extend our interpretation of complexes **1–3** as products of asymmetric Si–H addition and show that the stage of asymmetric oxidative addition is largely controlled by the substitution pattern at the five-coordinate silicon atom; and in particular by the ligand *trans* to the η^2-SiH moiety. Our model systems serve once again as benchmarks, containing as they do ligands (H or F) of a different chemical nature in the *trans* position, while the distorted trigonal bipyramidal geometry at Si remains invariant [H(1)–Si–H(2)/F = 148.5(8) and 148.8(2)$^\circ$ for **1** and **2**, respectively]. The Si–X bonds *trans* to the (η^2-SiH) moiety in **1** and **2** are elongated (by 0.02 and 0.08 Å, respectively) relative to those in SiH_4[13a] and SiF_4.[16] Such an elongation was first identified by Crabtree and Hamilton and interpreted in terms of σ(Mn–H) → σ^*(Si–X) donation, which is more pronounced for X = F or Cl than for X = H since the more electronegative the substituent at Si, the greater the Si character in the corresponding

σ*(Si–X) orbital and the greater the σ(Mn–H) → σ*(Si–X) charge transfer.[1c] However, such an explanation implies a concomitant weakening of the Mn–H bond in the fluoro complex **2** relative to the hydrido complex **1**, which is not evident in the precise crystal structures depicted in Fig. 1. Only the slightly endocyclic Mn–H and Si–H bond paths provide some indication that the metal hydride may be involved in charge transfer towards the Si atom.[3] In order to discount effects due to perturbation of the Mn–Si–H moiety in the crystal, we sought direct structural information for **1** and **2** in solution—the phase in which chemistry and catalysis occur. For Mn hydrides, intramolecular proton–proton and proton–metal dipole–dipole interactions dominate spin–spin relaxation of the hydride ^{1}H nucleus; hence Mn–H distances may be estimated accurately in solution by T_1 measurements.[17]

We have applied this methodology to **1** and **2**, and find excellent agreement between crystalline and solution phases: the T_1 NMR experiments yield a value of 1.56(3) Å for the Mn–H bond in each case,[4] identical within the range of experimental error with those deduced by neutron diffraction (*q.v.*) and complementary DFT calculations (1.565 and 1.566 Å for **1** and **2**, respectively). We conclude that there is no evidence for any structural difference between the Mn–H moieties in these two complexes.

However, a combined experimental and theoretical analysis of the CD distribution is superior to a simple geometrical analysis in revealing the subtle charge transfer occurring from the (η^2-SiH) moiety to the *trans* Si–H or Si–F ligand in **1** and **2**. Fig. 3 clearly reveals that the bonded charge concentrations in the valence shell of silicon in the region of the Si–Mn and Si–H bonds have merged into a singularity, denoted CC1 in the $L(\mathbf{r})$ map of **2**. Such a phenomenon is characteristic of electron delocalisation,[2c] and is the author of the unusual topology of the Si–H bond path, which appears to be attracted by the valence CC1 at the Si atom. Hence, as also revealed by the contour lines of the $L(\mathbf{r})$ distribution, the charge density associated with the hydridic hydrogen atom is strongly polarised not only towards the Mn atom, but also to a significant extent towards the electron-deficient Si centre. This H → Si charge transfer partially compensates for the pronounced polarisation of the Si–F bond, and results in a bonding scenario closely related to the negative (or anionic) hyperconjugation common in hypercoordinate silicon compounds. As pointed out by Schleyer *et al.*, such anomeric effects operate at silicon in spite of its electropositivity, and are responsible for the increased conformational flexibility of silicon compounds relative to their carbon analogues.[18] Thus, it is the electron-withdrawing character of the substituents *trans* to the Si–Mn bond, which control the extent of Mn–Si bonding in Mn(η^2-SiH) complexes.

To summarise our findings: the bonding in complexes **1** and **2** is not fundamentally different from that in systems like [Cp′Mn(CO)$_2$(η^2-HSiCl$_3$)] **3**, which possess more than one electronegative ligand at Si. These display shorter Mn–Si bonds with a slightly higher value of $\rho(\mathbf{r})$ at the BCP, but the Si–H interaction is not significantly weaker than that in **1** and **2**. The bonding situation in all of these complexes is naturally accommodated by an *asymmetric* oxidative addition reaction coordinate in which the Mn–H bond is formed at an early stage, while the establishment of the Mn–Si bond is controlled and enforced by the extent of charge transfer from the hydridic hydrogen atom to electronegative substituents at the hypervalent silicon atom.

This work was supported by the SPP1178 of the Deutsche Forschungsgemeinschaft, and by the NSERC of Canada.

Notes and references

1 (*a*) G. J. Kubas, *Acc. Chem. Res.*, 1988, **21**, 120; (*b*) M. Brookhart and M. L. H. Green, *J. Organomet. Chem.*, 1983, **250**, 395; (*c*) R. H. Crabtree and D. G. Hamilton, *Adv. Organomet. Chem.*, 1988, **28**, 299.

2 (*a*) W. Scherer, P. Sirsch, D. Shorokhov, M. Tafipolsky, G. S. McGrady and E. Gullo, *Chem.–Eur. J.*, 2003, **9**, 6057; (*b*) W. Scherer and G. S. McGrady, *Angew. Chem., Int. Ed.*, 2004, **43**, 1782; (*c*) W. Scherer, P. Sirsch, D. Shorokhov, G. S. McGrady, S. A. Mason and M. Gardiner, *Chem.–Eur. J.*, 2002, **8**, 2324.

3 U. Schubert, *Adv. Organomet. Chem.*, 1990, **30**, 151 and references therein.

4 G. S. McGrady, P. Sirsch, W. Scherer, G. Eickerling, N. P. Chatterton and A. Ostermann, *Organometallics*, submitted for publication.

5 U. Schubert, K. Ackermann and B. Wörle, *J. Am. Chem. Soc.*, 1982, **104**, 7378.

6 (*a*) N. K. Hansen and P. Coppens, *Acta Crystallogr., Sect. A*, 1978, **34**, 909; (*b*) T. Koritsánszky, S. Howard, T. Richter, Z. W. Su, P. R. Mallinson and N. K. Hansen, *XD Program*, Free University of Berlin, Germany, 1997.

7 Crystal data for **2**: $C_{20}H_{18}FMnO_2Si$, M_r = 392.37, white-yellow prisms; monoclinic, space group $P2_1/c$, a = 16.226(8), b = 7.032(3), c = 20.203(14) Å, β = 128.55(3)°, V = 1802.8(19) Å^3; T = 120(1) K; Z = 4, $F(000)$ = 808, D_{calc} = 1.446(2) g cm^{-3}, μ = 0.82 mm^{-1}. 177684 Bragg reflections were collected on a Nonius kappa-CCD system with a rotating anode generator (Nonius FR591; Mo-Kα, λ = 0.71073 Å); 19436 independent reflections; R_{int} = 0.037. The data set was corrected for beam inhomogeneity and absorption effects [T_{min}/T_{max} = 0.767(2)/0.838(2)]: 96% completeness in the data range $\sin\theta_{max}/\lambda$ = 1.11 Å^{-1}. The deformation density was described by a multipole model in terms of spherical harmonics multiplied by Slater-type radial functions with energy-optimised exponents (see ref. 8 and ESI†). During refinement the H atom positions and their anisotropic thermal parameters were fixed at the values obtained by another neutron diffraction study at 120 K from ref. 5 (see ESI†). The refinement of 601 parameters against 13961 observed reflections [$F > 3\sigma(F)$] converged to R_1 = 0.0207, wR_2 = 0.0599, GOF = 0.96, and a featureless residual $\rho(\mathbf{r})$. CCDC 604522. For crystallographic data in CIF or other electronic format see DOI: 10.1039/b604843a.

8 (*a*) E. Clementi and C. Roetti, *At. Data Nucl. Data Tables*, 1974, **14**, 177; (*b*) E. Clementi and D. L. Raimondi, *J. Chem. Phys.*, 1963, **38**, 2686.

9 Molecular geometries were fully optimised without any symmetry restraints at the BPW91/6-311G(d,p) level of approximation using Gaussian 98 (full citation in ESI†); the topology of $\rho(\mathbf{r})$ was analysed using a local version of the AIMPAC software package (ref. 11).

10 R. F. W. Bader, *Atoms in Molecules: A Quantum Theory*, Clarendon Press, Oxford, 1990.

11 F. W. Biegler-König, R. F. W. Bader and T. Tang, *J. Comput. Chem.*, 1982, **3**, 317.

12 (*a*) D. L. Lichtenberger and A. Rai-Chaudhuri, *J. Am. Chem. Soc.*, 1990, **112**, 2492; (*b*) D. L. Lichtenberger, *Organometallics*, 2003, **22**, 1599.

13 (*a*) D. R. Boyd, *J. Chem. Phys.*, 1955, **23**, 922; (*b*) M. J. Bearpark, G. S. McGrady, P. D. Prince and J. W. Steed, *J. Am. Chem. Soc.*, 2001, **123**, 7736.

14 S. J. La Placa, W. C. Hamilton, J. A. Ibers and A. Davison, *Inorg. Chem.*, 1969, **8**, 1928.

15 R. F. Bader and C. F. Matta, *Organometallics*, 2004, **23**, 6253.

16 J. Breidung, J. Demaison, L. Margules and W. Thiel, *Chem. Phys. Lett.*, 1999, **313**, 713.

17 V. I. Bakhmutov, J. A. K. Howard, D. A. Keen, L. G. Kuzmina, M. A. Leech, G. I. Nikonov, E. Vorontsov and C. C. Wilson, *J. Chem. Soc., Dalton Trans.*, 2000, 1631.

18 A. E. Reed, C. Schade, P. v. R. Schleyer, P. V. Kamath and J. Chandrasekhar, *J. Chem. Soc., Chem. Commun.*, 1988, 67.

